

A Versatile Processing Chain for Experimental TanDEM-X Product Evaluation

Marc Rodriguez-Cassola, Pau Prats, Luca Marotti, Matteo Naninni, Marwan Younis, Gerhard Krieger, and Andreas Reigber

Microwaves and Radar Institute, DLR, 82234 Wessling, Germany

Abstract

TanDEM-X is a high-resolution interferometric mission with the main goal of providing a global digital elevation model (DEM) of the Earth surface by means of single-pass X-band SAR interferometry. It is, moreover, the first genuinely bistatic spaceborne SAR mission, and, independently of its usual quasi-monostatic configuration, includes many of the peculiarities of bistatic SAR. An experimental, versatile, and flexible interferometric chain has been developed at DLR Microwaves and Radar Institute for the scientific exploitation of TanDEM-X data acquired in non-standard configurations. The paper describes the structure of the processing chain and focusses on some essential aspects of its bistatic part.

1 Introduction

TanDEM-X is the first bistatic SAR mission in space [1]. The main objective of the mission is to act as a single-pass interferometric system capable of providing very high resolution 3D information. As it is widely recognised, bistatic SARs offer increased performance at an increased operational cost. The uniqueness of the mission, coupled with the flexibility of the TerraSAR-X and TanDEM-X satellites, allows one to develop a large amount of challenging experiments to take advantage of the potential of the system. For the evaluation of these experiments, a flexible interferometric chain is being developed at DLR-HR to exploit the novel scientific data which will be gathered during the mission.

The paper addresses the particular characteristics of the processing chain, especially focussed on its bistatic part. Firstly, the TanDEM-X baseline model and the expected configurations are presented, followed by a block diagram of the processing chains. A discussion of the core of the bistatic processing part, with the selected synchronisation approach, imaging modes and processing kernels is also presented, including a performance analysis as a function of the key parameters of the system.

2 TanDEM-X baseline model

Considering the motion of the two satellites, TerraSAR-X and TanDEM-X move forming a helix in space to provide both varying across-track and along-track baselines and still have a negligible satellite collision probability. Expressed in the local coordinates of the TerraSAR-X satel-

lite, the TanDEM-X baseline can be approximated as

$$\Delta x(t) = \Delta x_0 + 2 \cdot A \cdot \sin[\phi_{\text{lat}}(t) + \alpha] \quad , \quad (1)$$

$$\Delta y(t) = -B \cdot \cos[\phi_{\text{lat}}(t)] \quad , \quad (2)$$

$$\Delta z(t) = -A \cdot \cos[\phi_{\text{lat}}(t) + \alpha] \quad , \quad (3)$$

where Δx_0 is a constant along-track offset, A is the maximum variation of the vertical across-track offset, B is the maximum variation of the horizontal across-track offset, ϕ_{lat} is the argument of latitude, and α is a constant angle representing the decoupling of the instant at which the maximum along-track offset and maximum across-track offset are reached. The x -axis of the local coordinates coincides with TerraSAR-X velocity vector, the z -axis is defined by the radial vector of the satellite position, being the y -axis the one to complete the coordinate axes. The baseline draws respective ellipses on the xy and xz planes, so that if the projections of the satellites on the xz plane are close, their respective projections on the xy plane are far, and *vice versa*. The baseline also changes mildly within an acquisition.

3 TanDEM-X during the commissioning phase

The main goal of the mission is the generation of the global DEM following the HRTI-3 standard [1]. The mission works on a tight schedule and, therefore, the baselines between the end of the commissioning phase until the beginning of mission's third year are usually not easily modifiable. From the third year onwards, the more demanding experiments and configurations are foreseen. An accelerated TerraSAR-X-like commissioning phase has been designed for the TanDEM-X satellite, before any bistatic operation is undergone. During this time, TerraSAR-X and

TanDEM-X satellites approach each other in order to prepare the close flying formation. Bistatic acquisitions with large along-track baselines (about 20 km) are foreseen during this commissioning phase to test the bistatic capabilities of the system. During its operational period, TanDEM-X will have baselines below 1 km. For the last stage of the mission, novel experiments with longer baselines are foreseen.

4 TAXI: TanDEM-X Interferometric Processor

The **TanDEM-X** interferometric processor for the evaluation of experimental data products which is being developed at DLR-HR, commonly known as TAXI, is a versatile SAR processing chain mainly composed of three main branches: a) a high-precision spaceborne monostatic part for the processing of TerraSAR-X data, b) a high precision spaceborne bistatic part for the processing of TanDEM-X data, and c) an interferometric part for the combination of two input images, either single pass or repeat pass, DEM generation and geocoding. Fig. 1 shows the block diagram of TAXI with its three main blocks.

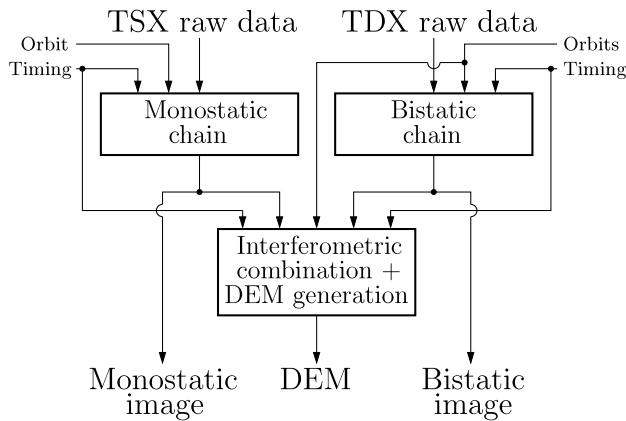


Figure 1: Block diagram of TAXI.

The standard imaging modes of TerraSAR-X are stripmap, sliding spotlight, and scanSAR, while TOPS is operated by DLR Microwaves and Radar Institute (DLR-HR) as an experimental mode [2]. Due to the usually quasi-monostatic configurations of TanDEM-X, analogous imaging modes extended to the bistatic case can be thought of. The focussing kernels of the monostatic part are based on the chirp scaling approach. The so-called extended chirp scaling (ECS) [3] is used for the stripmap configurations, whereas the other monostatic modes, which demand a special azimuth focussing approach, further use the common kernel of the baseband azimuth scaling (BAS) [2]. The interferometric part is composed of geometric+data-based coregistration, interferogram computation, phase unwrapping and DEM generation and geocoding. Repeat-pass in-

terferometry using TAXI has been demonstrated with all TerraSAR-X imaging modes including TOPS [4].

5 TAXI bistatic processing chain

TAXI's bistatic chain is a general azimuth-invariant bistatic SAR processor. Its block diagram is shown in Fig. 2. The basic structure consists of a synchronisation/calibration part and a focussing part. A feedback loop to estimate the residual synchronisation information has been included. This strategy is expected to be very useful in the experimental cases where the SNR of TanDEM-X synchronisation pulses might degrade the performance of the synchronisation link.

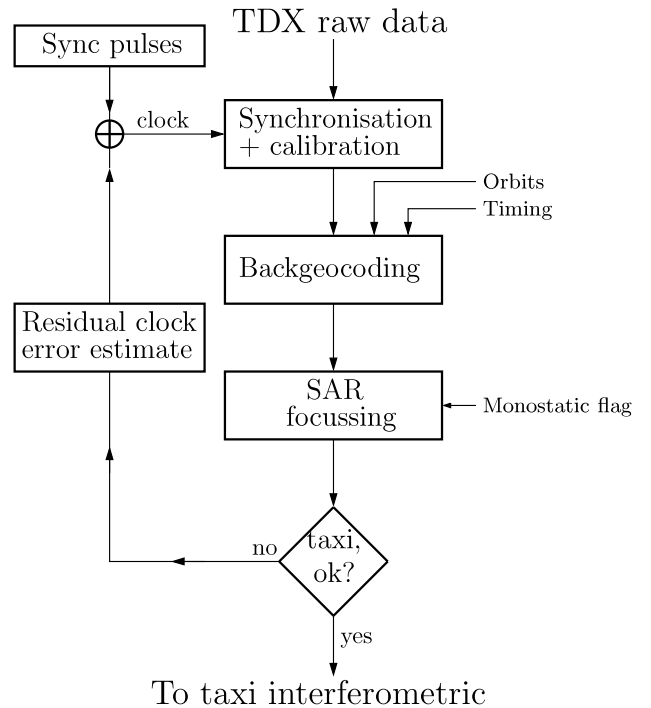


Figure 2: Block diagram of the bistatic part of the TanDEM-X interferometric processor.

5.1 Bistatic data synchronisation

TanDEM-X is a cooperative system. During the acquisitions, the TerraSAR-X and TanDEM-X satellites exchange transmitting pulses along their direct path for synchronisation purposes. An evaluation of these pulses provides information on the clock phase error, namely the frequency offset and the phase noise. This information is used for the synchronisation of the bistatic data, a crucial step if low-error interferograms are desired [1]. As expected, the higher the SNR of the synchronisation pulses (closer baselines, low antenna patterns attenuation) and the lower their pulse repetition interval, the lower the error in the estimation of the clock phase error. Due to the particularities

of the large baseline configurations, a significant decrease in the signal-to-noise ratio of the synchronisation pulses is expected and therefore a further automatic algorithm is foreseen. The automatic synchronisation is based on a direct comparison of the error-free monostatic image and the bistatic one. By measuring the deformation of this bistatic image, an estimate of the residual clock phase error can be obtained [6]. Fig. 3 shows the expected accuracy of the automatic synchronisation as a function of the duration of the acquisition and of the SCR of the image. The plot is optimistic, since it is assumed that non-coherent correlation is assumed along the swath for all azimuth blocks. if only one fourth of the range bins could be averaged the accuracy of the measure would worsen by a factor two.

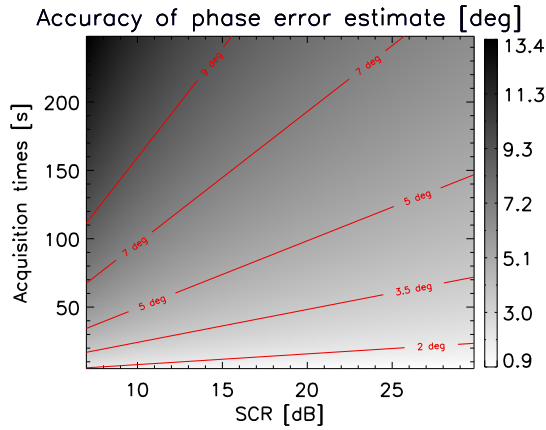


Figure 3: Accuracy of the phase error estimation as a function of the SCR and the duration of the data take. Non-coherent image combination.

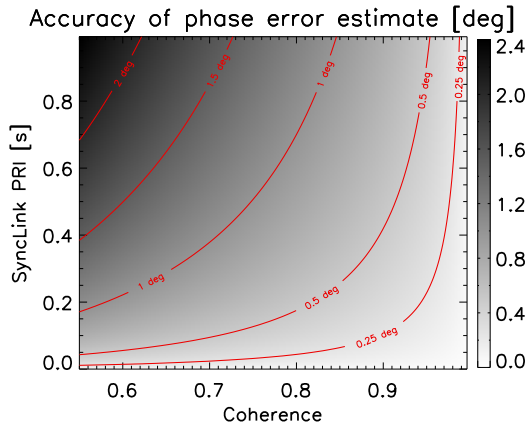


Figure 4: Accuracy of the phase error estimation as a function of the SyncLink pulse repetition interval (PRI) and scene coherence.

In fact, this automatic synchronisation can be also used in the case of smaller baselines where synchronisation pulses and coherence between the bistatic and monostatic images

might be available to reduce the PRF of the synchronisation link. Fig. 4 shows the accuracy of the automatic synchronisation as a function of the synchronisation link PRI and of the scene coherence. For an accuracy of the clock phase error estimate better than 1 deg, the synchronisation link PRF can be set to 5 Hz for practical purposes.

5.2 Bistatic SAR focussing

TerraSAR-X and TanDEM-X satellites fly in a quasi-azimuth-invariant configuration. Therefore, a Doppler-domain focussing approach is selected. Among the Doppler-domain options for the processing of spaceborne SAR data, a dual-solution approach is used for the bistatic focussing kernels. One option is to tune the monostatic processing functions so that they are matched to the bistatic configuration and then use the regular monostatic kernels, i.e., still using the hyperbolic approximation with an effective velocity [7]. Another one is to generate actual bistatic processing functions using a numerical approach [8]. The numerical solution is more cumbersome and usually increases the duration of the focussing part by a factor 2 to 3. Fig. 5 shows the maximum phase error at the edge of the synthetic aperture for a high-resolution spotlight acquisition for different combinations of across-track and along-track baseline. Whereas the impact of the across-track baseline is mild, an edge error better than 1 deg is expected for the operational configurations of the mission, the along-track baseline has a higher impact on the validity of the approximation.

Phase error hyperbolic approximation for HR spot [deg]

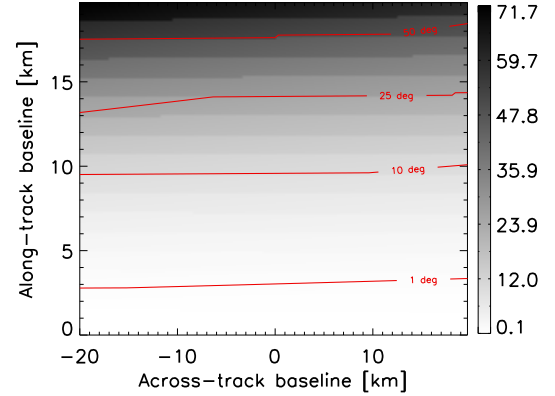


Figure 5: Maximum phase error at the edge of the synthetic aperture by using the hyperbolic monostatic approximation for a high-resolution spotlight case computed for near range.

The imaged scene, including topography, is backgeocoded in the bistatic radar coordinates, a step which is required for focussing and for the geometrical coregistration of the images during interferometric processing. Looking back to equations (1)-(3) describing TanDEM-X baseline, it is easy to see that it is not constant during the acquisition. In pu-

ity, TerraSAR-X and TanDEM-X fly in a bistatic azimuth-variant configuration. However, in practical terms, the change of the baseline within one data take is very slow, so we can assume the configuration to be invariant (i.e., the same azimuth processing functions can be used) for a certain scene size. If the along-track size of the data take exceeds this invariant scene size, azimuth block processing is required. TAXI's bistatic chain includes an azimuth-invariance check module to dynamically adapt the block scene size to that of the invariance region of the configuration. Fig. 6 shows the evolution of the maximum phase error at the edge of the synthetic aperture along the image block size for a stripmap acquisition with parameters $\Delta x_0 = 20$ km, $B = 20$ km, and $A = 5$ km.

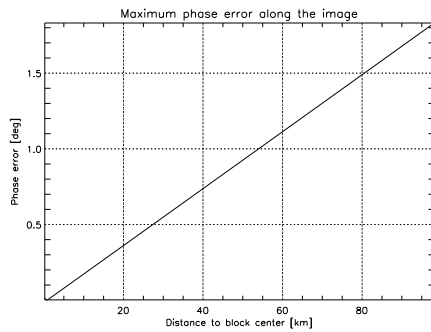


Figure 6: Evolution of the maximum phase error at the edge of the synthetic aperture along the image. Stripmap with $\Delta x_0 = 20$ km, $B = 20$ km, and $A = 5$ km

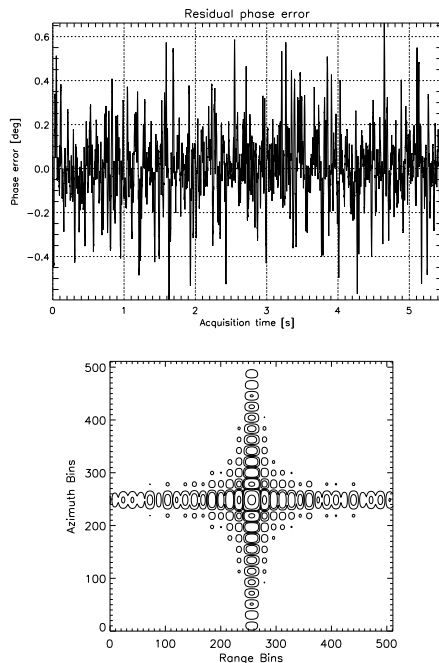


Figure 7: Residual phase error (top) after synchronisation (only using synchronisation pulses of 20 dB SNR). Point target contour (bottom) of a simulated point target processed using TAXI's bistatic processor.

Fig. 7 shows two significant outputs of TAXI's bistatic chain, obtained with realistic simulated raw data. A realistic clock phase error has been introduced in the raw data of a simulated point target. Synchronisation pulses have been generated and evaluated using TAXI, after which the residual clock phase error and the contour of the processed point target can be seen.

6 Summary

TAXI, the versatile interferometric processing chain for experimental TanDEM-X product evaluation of DLR-HR has been presented, with a special focus on the bistatic processing chain. Performance figures on different aspects of the synchronisation and focussing modules have also been addressed.

References

- [1] G. Krieger *et al.*, 'TanDEM-X: a satellite formation for high-resolution SAR interferometry', *IEEE Trans. Geosci. Remote Sens.*, vol. 45, no. 11, pp. 3317-3341, Nov. 2007.
- [2] P. Prats *et al.*, 'Processing of Sliding Spotlight and TOPS SAR Data Using Baseband Azimuth Scaling', *IEEE Trans. Geosci. Remote Sens.*, vol. 48, no. 2, pp. 770-780, Feb. 2010.
- [3] A. Moreira *et al.*, 'Extended chirp scaling algorithm for air- and spaceborne SAR data processing in stripmap and scansar imaging modes', *IEEE Trans. Geosci. Remote Sens.*, vol. 34, no. 5, pp. 1123-1136, Sep. 1996.
- [4] P. Prats *et al.*, *TOPS Interferometry with TerraSAR-X*, Proc. EUSAR 2010, Aachen, Germany.
- [5] M. Younis *et al.*, 'Performance Prediction of a Phase Synchronization Link for Bistatic SAR', *IEEE Geosci. Remote Sens. Lett.*, vol. 3, no. 3, pp. 429-433, Jul. 2006.
- [6] M. Rodriguez-Cassola *et al.*, *General processing approach for bistatic SAR systems: description and performance analysis*, Proc. EUSAR 2010, Aachen, Germany.
- [7] R. Bamler *et al.*, 'Processing of bistatic SAR data from quasi-stationary configurations', *IEEE Trans. Geosci. Remote Sens.*, vol. 45, no. 9, pp. 3350, Nov. 2007.
- [8] Y. L. Neo *et al.*, 'A two-dimensional spectrum for bistatic SAR processing using series reversion', *IEEE Geosci. Remote Sens. Lett.*, vol. 4, no. 1, pp. 93-96, Jan. 2007.